http://www.jstage.jst.go.jp/browse/biophysics

BIOPHYSICS

Vol. 6, pp. 37–51 (2010)
doi: 10.2142/biophysics.6.37

Modeling of the gap junction of pancreatic β-cells and the robustness of insulin secretion

Tomoki Kitagawa[1], Noriaki Murakami[1] and Seido Nagano[1]

[1]*Department of Bioinformatics, Ritsumeikan University, 1-1-1 Nojihigashi, Kusatsu, Shiga 525-8577, Japan*

Received 27 November, 2009; accepted 19 February, 2010

Pancreatic β-cells are interconnected by gap junctions, which allow small molecules to pass from cell to cell. In spite of the importance of the gap junctions in cellular communication, modeling studies have been limited by the complexity of the system. Here, we propose a mathematical gap junction model that properly takes into account biological functions, and apply this model to the study of the β-cell cluster. We consider both electrical and metabolic features of the system. Then, we find that when a fraction of the ATP-sensitive K^+ channels are damaged, robust insulin secretion can only be achieved by gap junctions. Our finding is consistent with recent experiments conducted by Rocheleau et al. Our study also suggests that the free passage of potassium ions through gap junctions plays an important role in achieving metabolic synchronization between β-cells.

Key words: pancreatic β-cells, gap junctions, synchronization, robustness

Synchronization of rhythms via receptors plays important roles in a variety of cellular processes. Cellular slime mold[1], in which rich quantitative experimental data are available, has played a significant role in studies of rhythm synchronization via cAMP receptors. A synchronization scheme developed for the cellular slime mold[2] has been generalized as a universal mathematical scheme[3–5]. Another important player in cellular synchronization is the gap junction. Most cells in animal tissues including pancreatic β-cells are in communication with their neighbors both electrically and metabolically via gap junctions, which allow the passage of small water-soluble ions and molecules smaller than ~ 1000 daltons. The phenomenon of synchronization via gap junctions in the pancreatic β-cells has been extensively investigated[6,7]. Nonetheless, the study of gap junctions is still in a challenging stage in large part because of the complex relationship between structure and function.

Pancreatic β-cells, located in the islets of Langerhans, secrete insulin in response to the level of glucose in the blood allowing the glucose level in the blood to be maintained within a small range around 5.6 mM. Insulin secretion is oscillatory with a period of ≤1 min (fast oscillatory mode), 2–7 min (slow oscillatory mode), or a combination of the two[8–10].

It is generally believed that Ca^{2+} feedback to ATP production is responsible for the fast oscillatory mode of insulin secretion, whereas glycolysis is responsible for the slow oscillatory mode. The glucose-phosphorylating enzyme glucokinase act as a metabolic glucose sensor in liver and β-cells[11]. The electrical activity of β-cells has a characteristic behavior known as bursting. A burst consists of an active phase of spiking followed by a silent phase of hyperpolarization. During the silent phase, Ca^{2+} is cleared by Ca^{2+} ATPases.

The essential processes in insulin secretion are as follows (see Fig. 1): ATP-sensitive K^+ channels in the plasma membrane are activated by ADP and inactivated by ATP; thus the ratio of these nucleotides determines the fraction of open K(ATP) channels. When the ATP/ADP ratio is elevated, there is a reduction in the number of open K(ATP) channels. This results in membrane depolarization, causing voltage-dependent Ca^{2+} channels to open. The resulting Ca^{2+} influx evokes insulin secretion. The difference among various mathematical models may originate in the extent to which

Corresponding author: Seido Nagano, Department of Bioinformatics, Ritsumeikan University, 1-1-1 Nojihigashi, Kusatsu, Shiga 525-8577, Japan. e-mail: nagano@sk.ritsumei.ac.jp

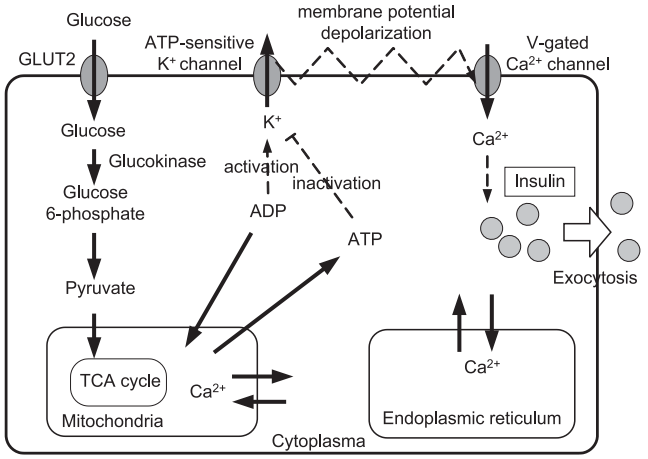

Figure 1 Essential processes of the insulin secretion[6]. Glucose is taken into the β-cell by GLUT-2 transporters, and broken down during glycolysis. Glycolytic product pyruvate is taken into the mitochondria in order to produce ATP. The ATP-sensitive K^+ channel regulates membrane potential, and Ca^{2+} flow into the cell, and the insulin release into the blood is prompted by the elevated cytosolic Ca^{2+} concentration.

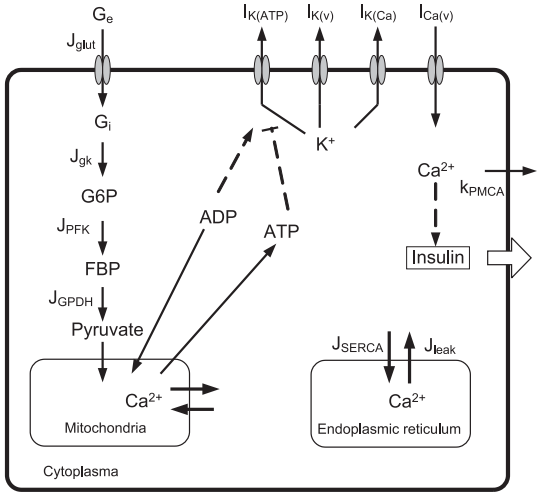

Figure 2 A scheme for insulin secretion adopted by Pedersen et al.[6] G_e is the extracellular glucose concentration; G_i is the intracellular glucose concentration; G6P is glucose 6-phosphate concentration; FBP is fructose 1-6-bisphosphate concentration; and SERCA means the SERCA pumps.

common cellular processes beyond the essential processes are taken into account.

Comparisons among experimental observations have been performed mostly in the context of mathematical models of single β-cells. However, experimental observations are conducted in β-cell clusters, where β-cells are connected with gap junctions. In this letter, we propose a gap junction model that clarifies the relationship between the synchronization phenomena and the cellular processes via gap junctions. From among many proposed single pancreatic β-cell models[6,10,12–20], here we adopt one by Pedersen et al.[6], and generalize their model from the single-cell level to a multicellular system. The model by Pedersen et al. (see Fig. 2) is not complete as a whole β-cell model, but its relative simplicity facilitates generalization to the multicellular system. We expect that the simplicity of the model can help our intuitive understanding of the numerical investigations. Naturally, this also gives some limitations to our study as discussed in Appendix A.

To model gap junctions, the electrical coupling between cells has often been handled by adding the following linear coupling term[6], $-g_c(v_i - v_j)$, where g_c is the coupling strength between neighbor cells i and j. Such a linear coupling approximation has recently been extended to Ca^{2+} and glycolytic metabolites[7]. In these works, the coupling strength of gap junctions has been treated as a free parameter while the relationship between the adopted coupling parameters and the structure and the function of gap junctions has been left as an unanswered question. Furthermore, the electrical coupling and the ion currents between β-cells must be studied in a consistent manner since ions such as K^+ and Ca^{2+} can freely move through gap junctions. Here, we propose a gap junction model based on the Goldman, Hogkin, and Katz (GHK) approximation[21] to answer such a fundamental question. Our proposed scheme can handle both the membrane ion currents and the gap currents in a consistent manner.

The structure of this paper is as follows. Following this brief introduction (Section I), we present our mathematical modeling of gap junctions in Section II, and describe our numerical investigations in Section III. Comparison of the prediction of our model to the recent experimental results of Rocheleau et al.[22] is presented in Section IV. Limitations of the linear coupling scheme are discussed in Section V. Finally, we discuss our results in Section VI.

Modeling of gap junctions of β-cells

We generalize the single β-cell model proposed by Pedersen et al to a multicellular system as follows. Our equation for the membrane potential (v) of the i-th β-cell is given by

$$C_m \frac{dv_i}{dt} + I^{(i)}_{K(v)} + I^{(i)}_{Ca(v)} + I^{(i)}_{K(Ca)} + I^{(i)}_{K(ATP)} = I^{(i)}_G, \qquad (1)$$

where C_m is the membrane capacitance, $I^{(i)}_{K(v)}$ is the v-dependent K^+ current, $I^{(i)}_{Ca(v)}$ is the v-dependent Ca^{2+} current, $I^{(i)}_{K(Ca)}$ is the calcium-activated K^+ current, $I^{(i)}_{K(ATP)}$ is the ATP-sensitive K^+ current, and $I^{(i)}_G$ is the gap current. Figure 3 shows the general structure of gap junctions. We also assume that the flow of ions through gap junctions is driven not only by the electric field but also by the concentration gradient. Thus, we obtain the Nernst-Planck equation for the flow of ions[21]

$$J_{G(A)} = -S_G D_A \left(\frac{dc_A}{dx} + \frac{z_A F c_A}{RT} \frac{d\phi}{dx} \right), \qquad (2)$$

where ϕ is the electrical potential, c_A is the concentration of type A ions, F is Faraday's constant, z is the valence of ions,

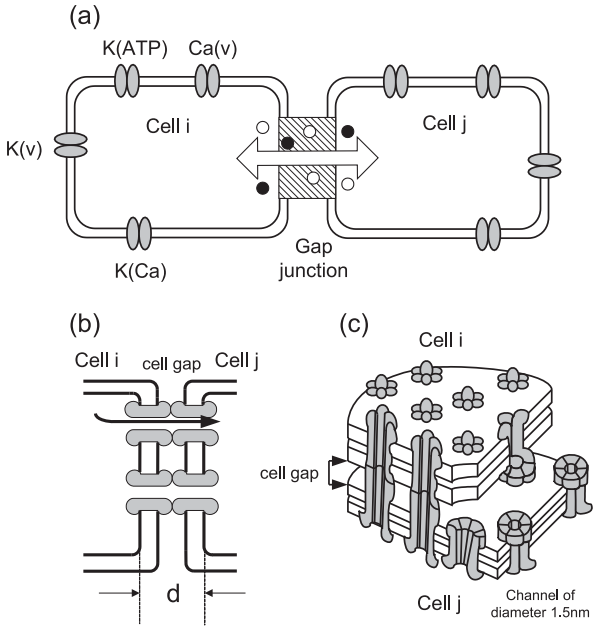

Figure 3 The general structure of gap junctions[23]. Within a gap junction, there are a few to many thousands channels of diameter 1.5 nm. The length of the cell gap is about 2~4 nm. The thickness of the cell membrane is about 5 nm. Thus, the length of the gap junctions d is nearly 13 nm. The channels allow inorganic ions and molecules with a mass of less than 1 kDa to pass into the other cell.

D_A is the diffusion constant of type A ions, S_G is the cross-sectional area of the gap junction, and RT is the gas constant multiplied by the absolute temperature. Then, the gap current I_G is

$$I_G = \sum_A z_A F J_{G(A)}.$$

We also use $S_G = \pi r_C^2 N_C$, where $r_C \cong 0.75$ nm is the radius of a single channel and N_C is number of channels in a gap junction. It is known that N_C is a few to many thousands[23]. When the length of the gap junctions is d (see Fig. 3b), the potential difference in the gap junction can be approximated (Goldman, Hogkin, and Katz[21]) as

$$\frac{d\phi}{dx} \cong \frac{(\phi^{(i)} - \phi^{(j)})}{d} = \frac{v_i - v_j}{d}.$$

Next, we obtain the following current equation of type A ions for the gap junctions

$$I_{G(A)}^{i \leftarrow j} = -\frac{D_A}{d}\frac{z_A^2 F^2}{RT} S_G (v_i - v_j) \frac{c_A^{(i)} - c_A^{(j)} \exp[-z_A F(v_i - v_j)/RT]}{1 - \exp[-z_A F(v_i - v_j)/RT]} \tag{3}$$

$$= -\frac{u_A}{d} z_A F S_G (v_i - v_j) \frac{c_A^{(i)} - c_A^{(j)} \exp[-z_A F(v_i - v_j)/RT]}{1 - \exp[-z_A F(v_i - v_j)/RT]}, \tag{4}$$

where the Einstein relation between the diffusion coeffcient D_A and the ionic mobility u_A, namely $D_A = u_A RT/z_A F$ is used. Thus, the gap current becomes

$$I_G^{(i)} = \sum_{j,A} I_{G(A)}^{i \leftarrow j}, \tag{5}$$

where j is the nearest-neighbor cell of cell i.

Using the gap current, the equation of conservation for K^+ ions within the i-th cell becomes

$$V_{cyt} \frac{dK^{(i)}}{dt} = \frac{1}{z_K F}[-I_{K(v)}^{(i)} - I_{K(Ca)}^{(i)} - I_{K(ATP)}^{(i)} + I_{K(in)}^{(i)} + I_{G(K)}^{(i)}], \tag{6}$$

where $V_{cyt} (= 1150(\mu m)^3)$ is the cytosolic volume of a single cell, $I_{K(in)}^{(i)}$ is the inward potassium current $I_{K(in)}^{(i)}$ (see Appendix A for its detailed discussion), and $I_{G(K)}^{(i)}$ is the gap current of K^+ ions. Summing the length of the cell gap (2~4 nm) and the thickness of the two neighboring cell membranes (~5 nm), we obtain $d = 3$ nm + 5 nm * 2 = 13 nm as an approximation here (see Fig. 3(b)). Such an approximation is necessary because the intracellular potential difference must vanish when the coupled system is in equilibrium.

Similarly, the equation of conservation for the free cytosolic Ca^{2+} concentration is

$$V_{cyt} \frac{dCa^{(i)}}{dt} = f_{cyt}\left[-\tilde{k}_{PMCA} Ca^{(i)} + J_{er}^{(i)} + \frac{1}{z_{Ca} F}(-I_{Ca(v)}^{(i)} + I_{G(Ca)}^{(i)})\right], \tag{7}$$

and the equation for the free Ca^{2+} concentration in the endoplasmic reticulum is

$$V_{er} \frac{dCa_{er}^{(i)}}{dt} = -f_{er} J_{er}^{(i)}, \tag{8}$$

where

$$J_{er}^{(i)} = \tilde{p}_{leak}(Ca_{er}^{(i)} - Ca^{(i)}) - \tilde{k}_{SERCA} Ca^{(i)}$$

is the Ca^{2+} flux out of the endoplasmic reticulum, $I_{G(Ca)}^{(i)}$ is the gap current of Ca^{2+}, f_{cyt} is the fraction of free to total cytosolic Ca^{2+}, and $\tilde{k}_{PMCA} \equiv k_{PMCA} V_{cyt}$, $\tilde{p}_{leak} \equiv p_{leak} V_{cyt}$, $\tilde{k}_{SERCA} \equiv k_{SERCA} V_{cyt}$. Where k_{PMCA}, k_{SERCA}, and p_{leak} are the PMCA pump rate, SERCA pump rate, and the Ca^{2+} leakage

Table 1 Typical variable values. See ref. 6 for other variables

Variables	
$C_m = 5300$ fF	$\bar{g}_K = 2700$ pS
$\bar{g}_{Ca} = 1000$ pS	$\bar{g}_{K(Ca)} = 400$ pS
$\bar{g}_{K(ATP)} = 40000$ pS	$v_K = -75$ mV
$v_{Ca} = 25$ mV	$V_{cyt} = 1150\ \mu m^3$
$V_{cyt}/V_{er} = 31$	$k_{PMCA} = 0.18\ ms^{-1}$
$k_{SERCA} = 0.4\ ms^{-1}$	$p_{leak} = 0.0002\ ms^{-1}$
$f_{cyt} = 0.01$	$f_{er} = 0.01$

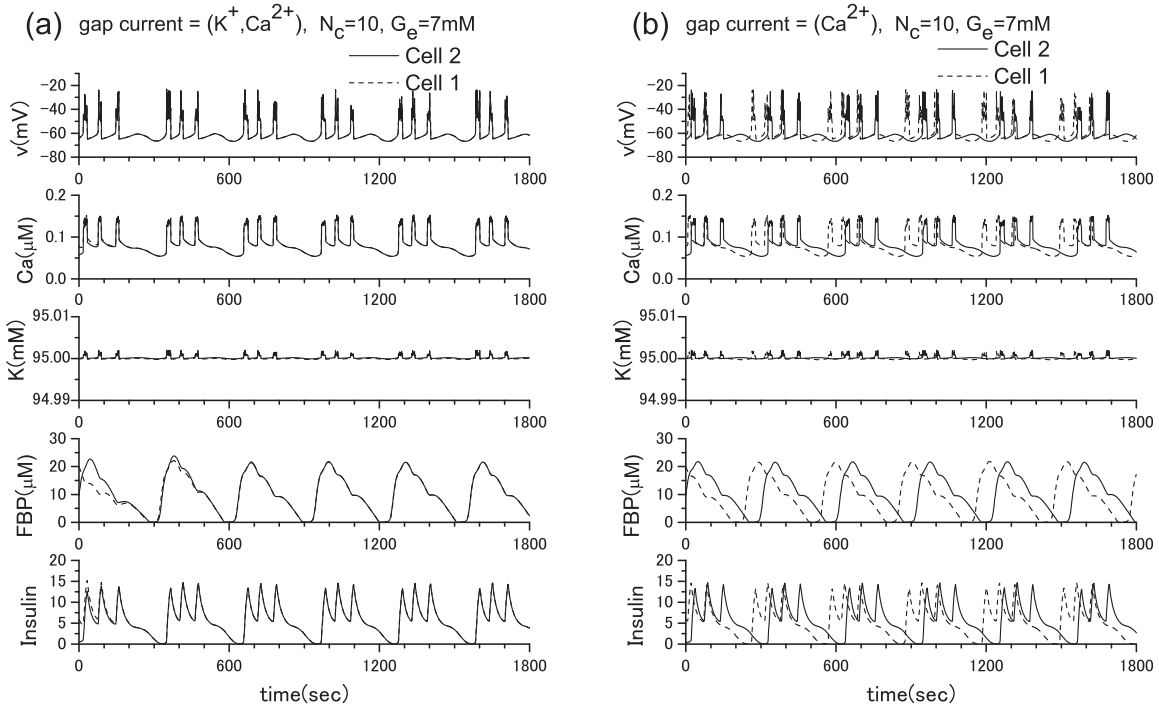

Figure 4 Synchronization is achieved immediately when both potassium ions and calcium ions are allowed to pass through gap junctions between two β-cells (a), but is not achieved when only calcium ions are allowed to pass through gap junctions (b). Here, $\bar{g}_{Ca}=1000$ pS, and $\bar{g}_{K(ATP)}=40000$ pS, and the extracellular glucose concentration is 7 mM. The solid line and dotted line indicate different β-cells.

rate from ER, f_{cyt} and f_{er} are the fraction of free to total cytosolic and the fraction of free to total ER Ca^{2+}, respectively, V_{er} is the volume of the ER compartment. Thus, we can handle gap junctions consistently.

Synchronization of beta-cells via gap junctions

To clarify the role of gap junctions in the cellular processes, we have conducted extensive numerical investigations. From many numerical experiments, first, we show the result for the two β-cell system in Fig. 4, where we adopt ionic mobilities in water at 298 K[24], namely, $u_K=7.62\times10^{-8}$ $m^2s^{-1}V^{-1}$, $u_{Ca}=6.17\times10^{-8}$ $m^2s^{-1}V^{-1}$ as an approximation since specific values for the ionic mobilities in the β-cells are not currently available to our knowledge. In Fig. 4(a), both K^+ ions and Ca^{2+} ions are allowed to pass through gap junctions. In this case, synchronization is achieved immediately although very different initial parameter values are adopted for the different cells. On the other hand, in Fig. 4(b), only Ca^{2+} ions are allowed to pass through gap junctions. It is clear that without free flow of K^+ ions through the gap junction, synchronization cannot be achieved. The result is reasonable since the K^+ ion concentration is much higher than the Ca^{2+} ion concentration within cells. Although we have also tested the case when only K^+ ions are allowed to pass through gap junctions, we do not show it here because the obtained figure is nearly identical to Fig. 4(a). For our next example, we show the result for the 100 β-cell system in Fig. 5, where the 10×10 square lattice with the periodic

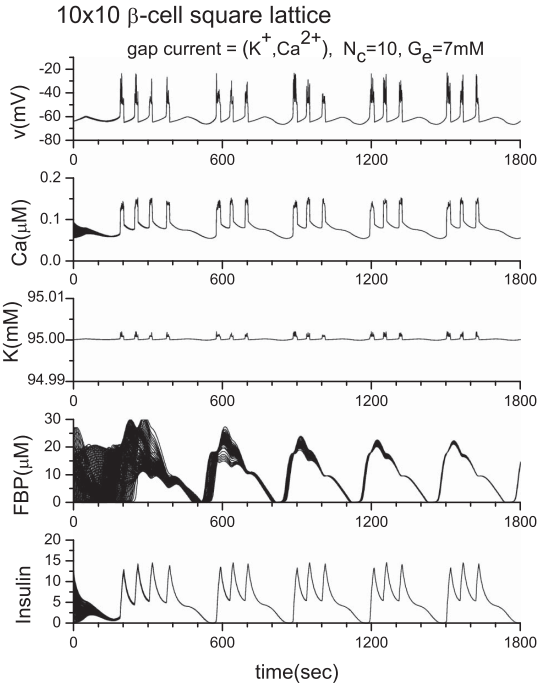

Figure 5 Synchronization of 10×10 β-cell square lattice with periodic boundary conditions. Here, $\bar{g}_{Ca}=1000$ pS, and $\bar{g}_{K(ATP)}=40000$ pS.

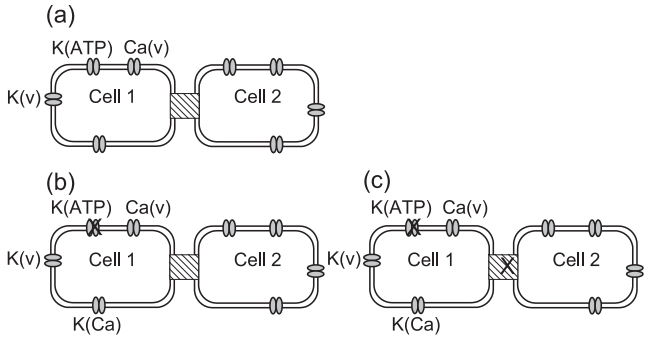

Figure 6 Two β-cells connected with gap junctions. (a) Wild type cells connected with gap junctions. (b) The K(ATP) channel in one of two β-cells is partially blocked. (c) The K(ATP) channel in one β-cell is blocked, and additionally, the gap junction is non-functional.

boundary condition is used. Once again, we observed synchronous bursting. We do not provide any figure of channel number dependence because no qualitative change was observed when N_c is changed from 1 to 100.

Robustness of the insulin secretion by gap junctions

Recently, Rocheleau et al.[22] conducted an interesting experiment by blocking the ATP-sensitive K^+ channels and gap junctions. They used transgenic mice and showed that the robust control of the insulin secretion can be achieved by the gap junctions. Following their experiment, we conducted a numerical experiment in which $G_e = 2$ mM. To simulate their experiment, we reduced the conductance of the ATP-sensitive K^+ channels by decreasing the value of $\bar{g}_{K(ATP)}$ from the original value of 40000 pS to 10000 pS in a single β-cell. In this case, the insulin secretion is prompted as shown in Fig. 15. This corresponds to the case where the gap junction is disconnected (case in Fig. 6(c)). If the ATP-sensitive K^+ channels are fully functional, no insulin secretion should be observed when $G_e = 2$ mM as shown in Fig. 13. However, when the gap junction is opened (case in Fig. 6(b)), insulin secretion ceases, as shown in Fig. 7(b). This robustness of the insulin secretion is consistent with the experiments of Rocheleau et al. To clarify the detailed mechanism of this robustness, we show the ATP-sensitive potassium current $I_{K(ATP)}$ and the gap currents $I_{G(K)}$ and $I_{K(Ca)}$ in Fig. 8. When the ATP-sensitive potassium channels of both cells are not blocked, the gap currents are negligibly small. However, when one of two cells is blocked, $I_{G(K)}$ and $I_{K(ATP)}$ of the normal cell ($\equiv I^{\text{normal}}_{K(ATP)}$) are significantly increased (see Figs. 8(b), 8(c)). Figure 8(d) shows that $I^{\text{normal}}_{K(ATP)}$ minus $I_{G(K)}$ is nearly equal to the $I_{K(ATP)}$ of the blocked cell ($\equiv I^{\text{blocked}}_{K(ATP)}$) plus $I_{G(K)}$. Besides, both values are roughly equal to $I_{K(ATP)}$ in equilibrium state in Fig. 8(a). This means that a significant increase of $I_{K(ATP)}$ of the normal cell is brought about mostly by the outward gap current $I_{G(K)}$ from the blocked cell. This increase of $I_{G(K)}$ brings the intracellular potassium density of the blocked cell back to the normal level, and the insulin

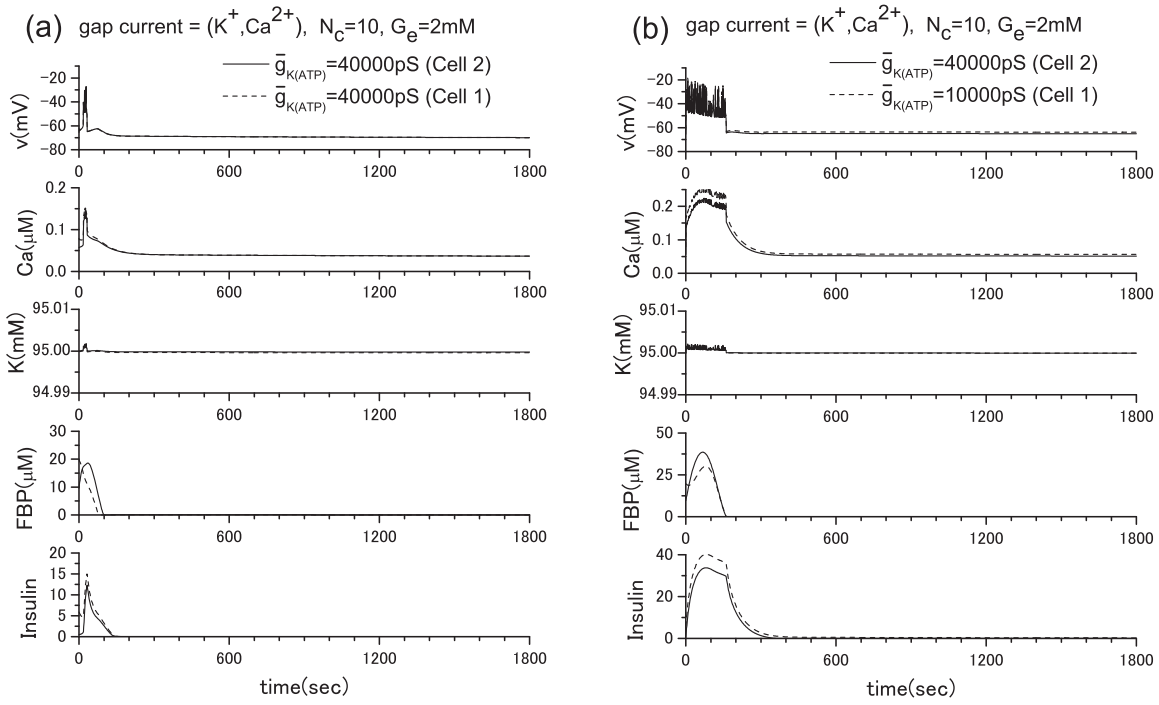

Figure 7 Partial blocking of the ATP-sensitive K^+ channels of the two β-cell system when $G_e = 2$ mM. (a) $\bar{g}_{K(ATP)} = 40000$ pS (Cell 2), 40000 pS (Cell 1), (b) $\bar{g}_{K(ATP)} = 40000$ pS (Cell 2), 10000 pS (Cell 1). The above figures correspond to the cases of Figs. 6(a) and 6(b), respectively. In the case of Fig. 6(c), the result becomes the simple sum of Fig. 14 and Fig. 15 since the gap junction is closed. This means that the insulin secretion cannot be stopped, even though the glucose level is low.

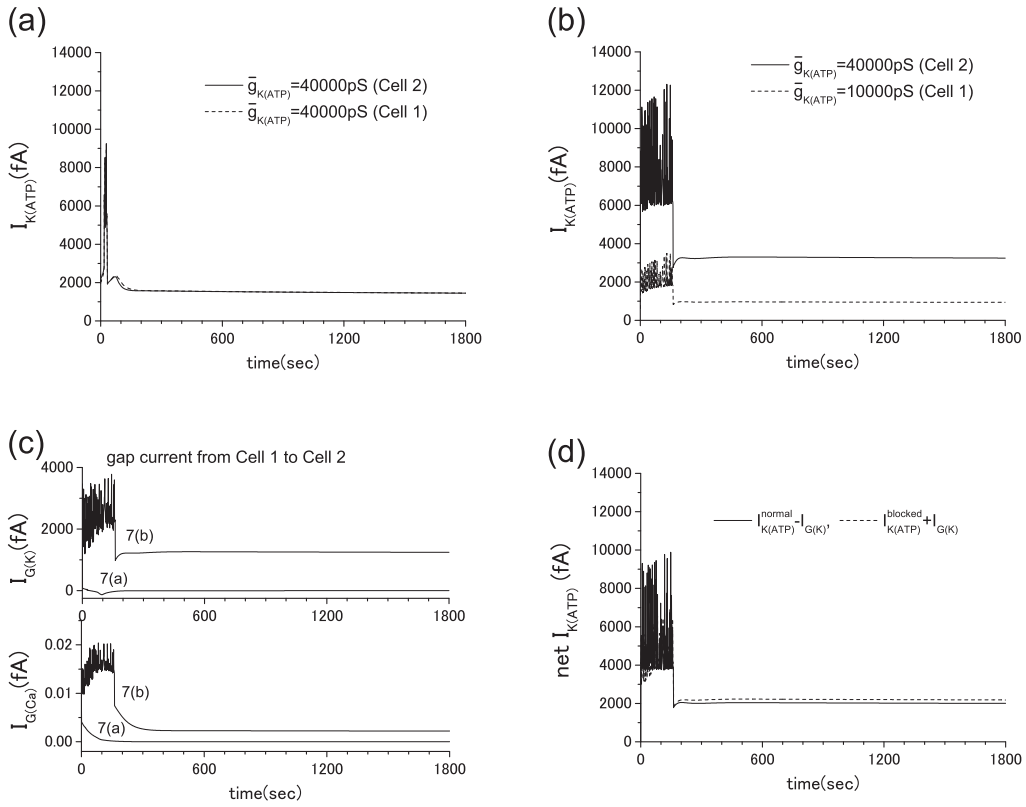

Figure 8 ATP-sensitive K^+ current and gap currents of the cases in Fig. 7, where G_e=2 mM. (a) $I_{K(ATP)}$ of the case of Fig. 7(a), (b) $I_{K(ATP)}$ of the case of Fig. 7(b), (c) gap currents $I_{G(K)}$ and $I_{G(Ca)}$ of the cases of Figs. 7(a) and 7(b). When the ATP-sensitive potassium channels of both cells are fully functional, the gap currents are negligibly small. However, when one of them is blocked, the outward gap currents from the blocked cell and $I_{K(ATP)}$ of the normal cell are significantly increased, (d) a comparison of $I^{\text{blocked}}_{K(ATP)}+I_{G(K)}$ and $I^{\text{normal}}_{K(ATP)}-I_{G(K)}$, where $I^{\text{blocked}}_{K(ATP)}$ and $I^{\text{normal}}_{K(ATP)}$ are ATP-sensitive potassium current of the blocked cell and that of the normal cell, respectively. Note that $I^{\text{blocked}}_{K(ATP)}+I_{G(K)}$ and $I^{\text{normal}}_{K(ATP)}-I_{G(K)}$ in Fig. 8(d) are roughly equal to $I_{K(ATP)}$ in Fig. 8(a). An increase of $I_{G(K)}$ brings the intracellular potassium density of the blocked cell back to the normal level, and ultimately the insulin secretion is ceased. The intercellular collaboration of ATP-sensitive potassium channels via gap junctions is a key of this robustness. Here the positive direction of $I_{K(ATP)}$ is outward from the cell.

secretion ceases. Namely, the intercellular collaboration of ATP-sensitive potassium channels via gap junctions is a key of this robustness. Here the positive direction of $I_{K(ATP)}$ is outward from the cell.

For the further confirmation of the above analysis, we have increased the extracellular glucose concentration G_e from 2 mM to 7 mM as shown in Fig. 9. Since we have already studied the case where both cells are normal as presented in Fig. 4(a), only the blocked case is shown in Fig. 9(e) except gap currents and $I_{K(ATP)}$.When G_e=7 mM, the insulin is constantly secreted, but the role of gap junction for the metabolic synchronization is still important when some cell is damaged.

To investigate the role of gap junctions further, we studies the activity of the voltagegated Ca^{2+} channel by changing $\bar{g}_{Ca}$ values. The original $\bar{g}_{Ca}$ value is 1000 pS, and Fig. 14 shows the model calculations. We then changed the value of $\bar{g}_{Ca}$ from 1000 pS to 900 pS and 1100 pS. Their corresponding results are shown in Figs. 16 and 17, respectively. Two coupled β-cells are successfully synchronized via the gap junction, and a very similar result to that of the $\bar{g}_{Ca}$ = 1000 pS case is produced (see Fig. 11(a) or Fig. 14) although original individual patterns are very different each other as shown in Figs. 16 and 17. This kind of character has been observed consistently in other tested cases including the three coupled β-cell system.

The linear coupling scheme and its limitations

Because of its mathematical simplicity, the linear coupling scheme is often adopted for handling gap junctions without detailed biological discussions. Here we derive it from Eq. (4). By using the condition, $c_A^{(i)}=c_A^{(j)}$ (i, j are neighbor cell numbers), we can obtain

$$\begin{aligned} I_G^{(i)} &= -\sum_A \frac{u_A}{d} z_A F c_A^{(i)} S_G \sum_j (v_i - v_j) \\ &= -g_c^{(i)} \sum_j (v_i - v_j), \end{aligned} \tag{9}$$

where $g_c^{(i)} = FS_G / d \sum_A u_A z_A c_A^{(i)}$. Here, we assume that only Ca^{2+} and K^+ ions go through gap junctions. Then,

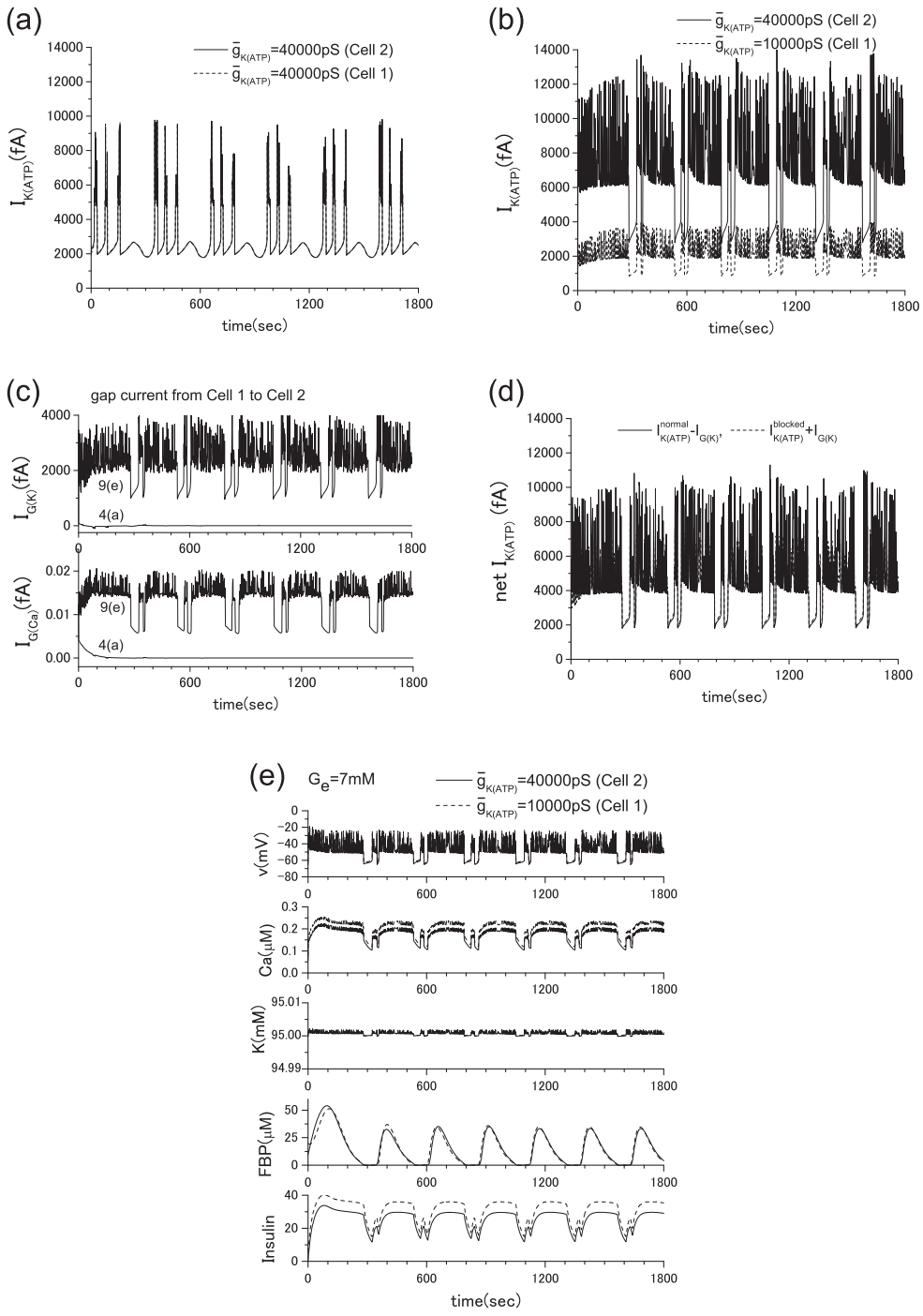

Figure 9 ATP-sensitive K^+ current and gap currents, where G_e=7 mM. Similar to Fig. 8, the blocked or damaged cell significantly increases the outward gap currents $I_{G(K)}$ and $I_{G(Ca)}$ from the cell. (a) $I_{K(ATP)}$ of the case of Fig. 4(a), (b) $I_{K(ATP)}$ of the case of Fig. 9(e), (c) gap currents $I_{G(K)}$ and $I_{G(Ca)}$ of the cases of Figs. 4(a) and 9(e). (d) a comparison of $I^{\text{blocked}}_{K(ATP)}+I_{G(K)}$ and $I^{\text{normal}}_{K(ATP)}-I_{G(K)}$. They are nearly identical and in the same range of value of $I_{K(ATP)}$ in equilibrium state (2000 fA~10000 fA) in Fig. 9(a).

$$I_G^{(i)} = I_{G(K)}^{(i)} + I_{G(Ca)}^{(i)} = -g_{c(K)}^{(i)} \sum_j (v_i - v_j) - g_{c(Ca)}^{(i)} \sum_j (v_i - v_j) . \quad (10)$$

Since $c_K/c_{Ca} >> 1$ within cells, it is clear that K^+ ions play a much more important role than Ca^{2+} ions in the coupling of β-cells by gap junctions. If we use c_K=95 mM, c_{Ca}= 5.5×10^{-2} μM, and T=310 K, we obtain $g_c \cong g_{c(K)}=95N_c$pS and $g_{c(Ca)}=1.1\times10^{-5}N_c$pS.

To clarify the limitation of the linear coupling scheme, we have conducted the following numerical experiments.

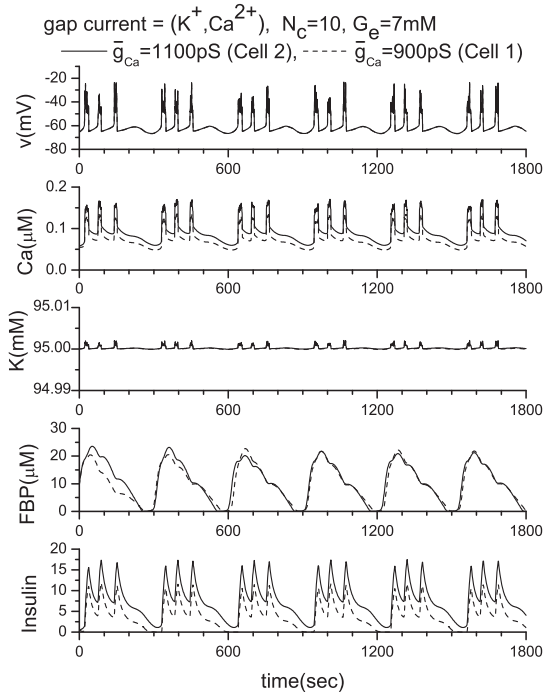

Figure 10 Two β-cells with different $\bar{g}_{Ca}$ values, where $\bar{g}_{Ca}$ = 1100 pS (Cell 2), 900 pS (Cell 1), and G_e = 7 mM.

The results are shown in Figs. 11 and 12, in which the number of channels is N_c = 10 as in previous investigations. By comparing Figs. 11(a) and 4(a), Figs. 11(b) and 10, and Figs. 12 and 7, it becomes clear that the linear coupling scheme works very well except when the $\bar{g}_{K(ATP)}$ values of individual β-cells are different as shown in Fig. 12(b). The variation of $\bar{g}_{Ca}$ values does not provide any problem as an approximation. This difference originates in how the intracellular potassium concentration is a ected by the parameter value variation. As shown in Fig. 15, only $\bar{g}_{K(ATP)}$ variation has a ected the intracellular potassium concentration significantly. As a consequence, the precondition of $c_K^{(i)} = c_K^{(j)}$ for this scheme is lost.

Discussion

In this study, we have proposed a mathematical model for the gap junction based on the biological functions and the structure of gap junctions, and applied it to the β-cell cluster in the islets of Langerhans. Our model demonstrates that free flow of potassium ions through gap junctions plays an essential role in achieving synchronous bursting. When metabolic synchronization between β-cells is achieved, the net current through gap junctions becomes negligible. However, the ionic flow through gap junctions becomes essential when some of the ATP-sensitive K^+ channels in the β-cells are damaged. The proved robustness of the insulin secretion is consistent with the experimental observations of Rocheleau et al.[22]. We offer the following interpretation of our findings. Intracellular calcium ion concentration is relatively insensitive to the variation of the conductance $\bar{g}_{Ca}$ so

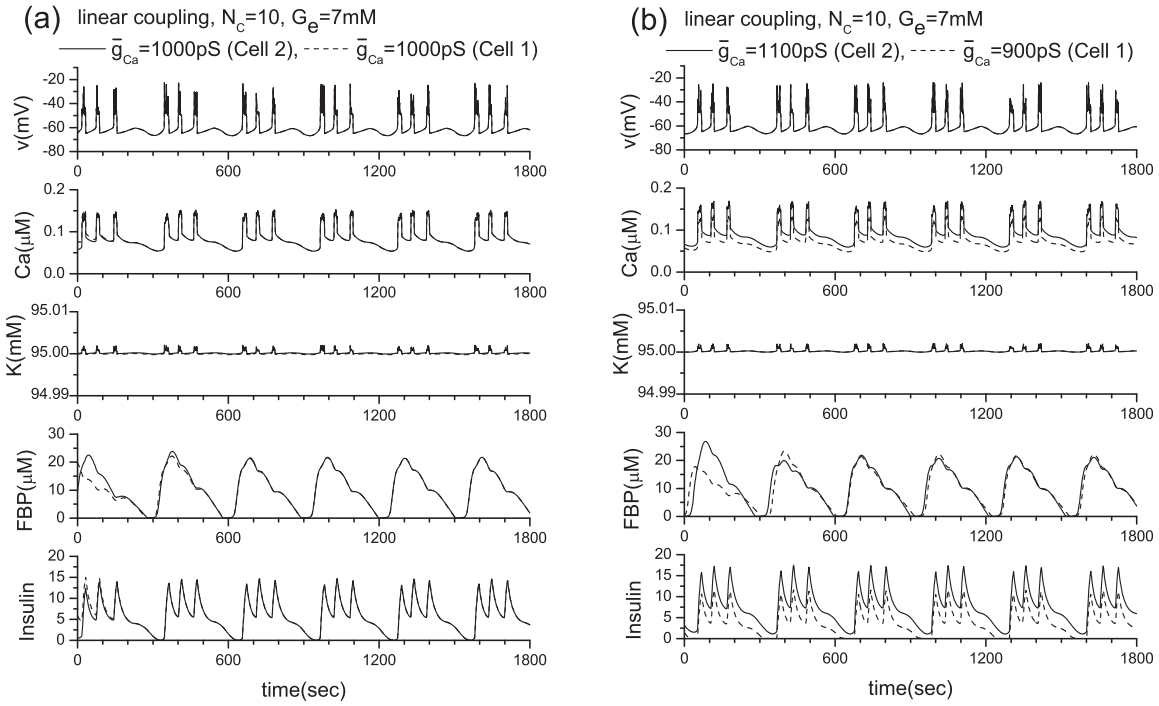

Figure 11 Results of the linear coupling scheme. Here, two β-cells with the same and different $\bar{g}_{Ca}$ values when G_e = 7 mM. (a) $\bar{g}_{Ca}$ = 1000 pS (Cell 2), 1000 pS (Cell 1), and (b) $\bar{g}_{Ca}$ = 1100 pS (Cell 2), 900 pS (Cell 1).

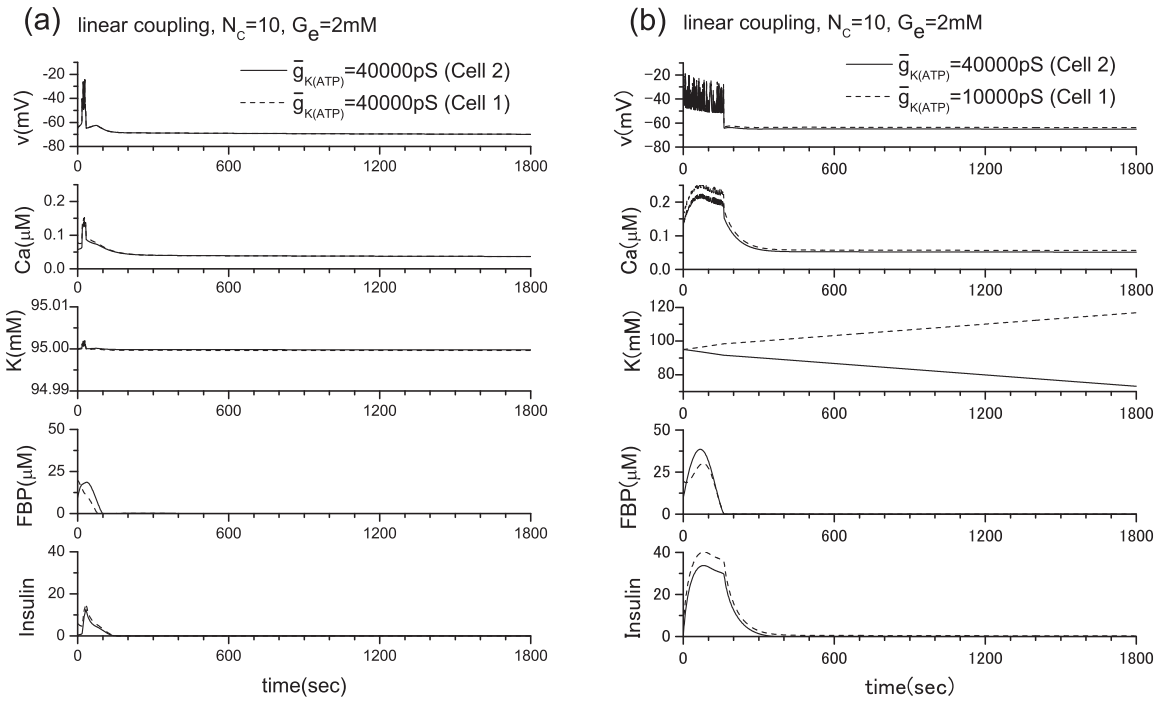

Figure 12 Results of the linear coupling scheme. Here, two β-cells with the same and different $\bar{g}_{K(ATP)}$ values when $G_e = 2$ mM. (a) $\bar{g}_{K(ATP)} = 40000$ pS (Cell 2), 40000 pS (Cell 1), (b) $\bar{g}_{K(ATP)} = 40000$ pS (Cell 2), 10000 pS (Cell 1).

long as the function of the ATP-sensitive K^+ channels is normal. However, when a fraction of the ATP-sensitive K^+ channels is damaged, intracellular potassium ion concentration is increased (Fig. 15). This increase also brings about an increase in calcium ion concentration. As a consequence, insulin secretion is stimulated even when the glucose level is low. However, when the damaged cell is connected with the normal cells with gap junctions, mutual membrane potential synchronization is achieved immediately due to the free flow of potassium ions through gap junctions. Thus, the intracellular potassium ion concentration of the damaged cell returns to the normal level, and calcium ion concentration is reduced to the normal level a little later. This stops insulin secretion, and the robust insulin secretion can be achieved (Figs. 7 and 8).

We have also derived a linear coupling scheme from the GHK approximation, assuming that the ion concentrations between neighbor cells are nearly equal. The performance of the linear coupling scheme is excellent, so long as the ATP-sensitive K^+ channels are normal between neighbor cells because the intracellular potassium density is sensitive to ATP-sensitive K^+ channels (Fig. 15). One cannot expect nearly equal ion concentrations between neighboring cells, as that would break the basis of the linear coupling scheme.

As discussed in Appendix A, we have introduced $I_{K(in)} = -I_{Ca(v)}$ term into the equation of conservation for potassium ions as an approximation. This mathematical (as opposed to biological) approximation is necessary to hold intracellular potassium concentration steady, in the context of the single β-cell model by Pedersen et al. and their original parameter values. This problem does not appear explicitly so far as the constant Nernt potential is adopted in any scheme. This inconsistency may have occurred due to the lack of pumps that are responsible for the inward potassium current in the model equations. Thus, in future models, we would like to introduce such pumps along with the sodium current in order to avoid such a drastic approximation. Until then, we should take our findings as predictions and they must be confirmed by the direct observation of gap currents.

Acknowledgments

We appreciate Professor Michael Meyer-Herman very much for sending us β-cell modeling software. We also appreciate Professor Sherman for sending us his preprint (Tsaneva-Atanasova and Sherman, Biophysical Journal **97**, November, 2009) after completion of the current work, and very extensive and constructive discussions. He has studied the same problem of Rocheleau et al.[22], too, by adopting the linear coupling model. We also acknowledge Mr. Atshushi Yokoyama for his help during the preparatory stages of the current work.

References

1. Nagano, S. Modeling the model organism *Dictyostelium discoideum*. *Develop. Growth Differ.* **42**, 541–550 (2000).
2. Nagano, S. Diffusion-assisted aggregation and synchroniza-

tion in *Dictyostelium discoideum*. *Phys. Rev. Lett.* **80**, 4826–4829 (1998).
3. Nagano, S. Biological receptor scheme for the robust synchronization of limit cycle oscillators. *Prog. Theor. Phys.* **107**, 861–877 (2002).
4. Nagano, S. Receptors as a master key for synchronization of rhythms. *Phys. Rev. E.* **67**, 0562151–0562154 (2003).
5. Yokoyama, A. & Nagano, S. Biological receptor scheme for the external synchronization of mutually coupled oscillator systems. *J. Phys. Soc. Jpn.* **77**, 0240021–0240029 (2008).
6. Pedersen, M. G., Bertram, R. & Sherman, A. Intra- and inter-islet synchronization of metabolically driven insulin secretion. *Biophys. J.* **89**, 107–119 (2005).
7. Tsaneva-Atanasova, K., Zimliki, C. L., Bertram, R. & Sherman, A. Diffusion of calcium and metabolites in pancreatic islets: killing oscillations with a pitchfork. *Biophys. J.* **90**, 3434–3446 (2006).
8. Bergsten, P. & Hellman, B. Glucose-induced amplitude regulation of pulsatile insulin secretion from individual pancreatic islets. *Diabetes* **42**, 670–674 (1993).
9. Bergsten, P. Slow and fast oscillations of cytoplasmic Ca^{2+} in pancreatic islets correspond to pulsatile insulin release. *Am. J. Physiol.* **268**, E282–E287 (1995).
10. Bertram, R., Satin, L. S., Pedersen, M. G., Luciani, D. S. & Sherman, A. Interaction of glycolysis and mitochondrial respiration in metabolic oscillations of pancreatic islets. *Biophys. J.* **92**, 1544–1555 (2007).
11. Baltrusch, S. & Tiedge, M. Glucokinase regulatory network in pancreatic β-cells and liver. *Diabetes* **55**, S55–S64 (2006).
12. Chay, T. R. & Keizer, J. Minimal model for membrane oscillations in the pancreatic β-cell. *Biophys. J.* **42**, 181–190 (1983).
13. Sherman, A., Rinzel, J. & Keizer, J. Emergence of organized bursting in clusters of pancreatic β-cells by channel sharing. *Biophys. J.* **54**, 411–425 (1988).
14. Smolen, P. & Keizer, J. Slow voltage inactivation of Ca^{2+} currents and bursting mechanisms for the mouse pancreatic beta-cell. *J. Membrane Biol.* **127**, 9–19.
15. Smolen, P. A model for glycolytic oscillations based on skeletal muscle phosphofructokinase kinetics. *J. Theor. Biol.* **174**, 137–148 (1995).
16. Maki, L. W. & Keizer, J. Analysis of possible mechanism for in vitro oscillations of insulin secretion. *Am. J. Physiol.* **268**, C780–C791 (1995).
17. Fridlyand, L. E., Tamarina, N. & Philipson, L. H. Modeling of Ca^{2+} flux in pancreatic β-cells: role of the plasma membrane and intracellular stores. *Am. J. Endocrinol.* **285**, E138–E154 (2003).
18. Bertram, R., Satin, L. S., Zhang, M., Smolen, P. & Sherman, A. Calcium and glycolysis mediate multiple bursting modes in pancreatic islets. *Biophys. J.* **87**, 3034–3087 (2004).
19. Bertram, R., Pedersen, M. G., Luciani, D. S. & Sherman, A. A simplified model for mitochondrial ATP production. *J. Theor. Biol.* **243**, 575–586 (2006).
20. Meyer-Hermann, M. E. The electrophysiology of the β-cell based on single transmembrane protein characteristics. *Biophys. J.* **92**, 2952–2968 (2007).
21. Keener, J. & Sneyd, J. *Mathematical Physiology.* Berlin: Springer (1998).
22. Rocheleau, J. V., Remedi, M. S., Granada, B., Head, W. S., Koster, J. C., Nichols, C. G. & Piston, D. W. *Plos Biol.* **4**, e26 (2006).
23. Alberts, B., Johnson, A., Lewis, J., Raff, M., Roberts, K. & Walter, P. *Molecular Biology of the Cell*. Garland Science. p. 1075 (2002).
24. Atkins, P. & Paula J. *Physical Chemistry Seventh Edition.* Oxford: Oxford Univ. Press. p. 1103 (2002).
25. Atwater, I., Ribalet, B. & Rojas, E. Cyclic changes in potential and resistance of the β-cell membrane induced by glucose in islets of Langerhans from mouse. *J. Physiol.* **278**, 117–139 (1978).

APPENDIX A

Modification of the single b-cell model by Pedersen et al.

In this letter, we adopt the single β-cell model by Pedersen et al., and their fitting parameters[6] unless stated otherwise (only typical parameters are shown in Table 1). However, for handling the ion flow through gap junctions, we must modify their model, although their original parameter values are not changed.

The equation for the membrane potential (v) of a β-cell is

$$C_m\frac{dv}{dt} + I_{K(v)} + I_{K(Ca)} + I_{K(ATP)} + I_{Ca(v)} = 0, \qquad \text{(A1)}$$

and the equation for the free cytosolic Ca^{2+} concentration is

$$V_{cyt}\frac{dCa}{dt} = f_{cyt}\left[-\tilde{k}_{PMCA}Ca + J_{er} - \frac{1}{z_{Ca}F}I_{Ca(v)}\right]. \qquad \text{(A2)}$$

For potassium, the approximation of constant K^+ ion concentration is used. But such an approximation is not appropriate to study the gap junctions. In general, the Nernst potential of the potassium, v_K, assumes the constant K^+ ion concentrations. A natural replacement of such an approximation is the adoption of the equation for the conservation of K^+ ions within a cell,

$$V_{cyt}\frac{dK}{dt} = \frac{1}{z_K F}[-I_{K(v)} - I_{K(Ca)} - I_{K(ATP)}], \qquad \text{(A3)}$$

where $K \equiv c_K$ is the intracellular K^+ ion concentration. However, Eq. (A3) does not guarantee stable K^+ ion concentration within a cell as shown in Fig. 13. This result is not consistent with the constant Nernst potential, either. This is because pumps that are responsible for the inward potassium current are not included in the scheme to stabilize the intracellular K^+ ion concentration. Then, we rewrite Eq. (A3) as

$$V_{cyt}\frac{dK}{dt} = \frac{1}{z_K F}[-I_{K(v)} - I_{K(Ca)} - I_{K(ATP)} + I_{K(in)}] \qquad \text{(A4)}$$

where $I_{K(in)}$ is the inward potassium current. But an introduction of the new term $I_{K(in)}$ should not break the consistency of the whole scheme. In the steady state, $dv/dt = dK/dt = 0$. Then, we can derive the relationship, $I_{K(in)} = -I_{Ca(v)}$, from Eqs. (A1) and (A4). We adopt it as an approximation in the near-equilibrium state. Figure 14 shows that this approximation can successfully stabilize the intracellular K^+ ion concen-

tration without breaking the self-consistency of the whole scheme. We use c_K=95 mM[25] as the intracellular K^+ ion concentration at the rest-cell state in the current calculations. An adoption of c_K=132.4 mM[17] instead of c_K=95 mM only shifts the base values of the K^+ ion concentration from 95 mM to 132.4 mM in every calculation. The inward potassium current has already been taken into account in the single β-cell models by Meyer-Hermann[20] in a different form.

For a wide range of studies of multicellular systems, it is necessary to confirm that our approximation, $I_{K(in)}=-I_{Ca(v)}$, does not produce any artificial e ect within the single β-cell system. Otherwise, the reliability of our study of multicellular systems could be lost. Therefore, we have conducted extensive numerical calculations by changing the values of $\bar{g}_{K(ATP)}$ and $\bar{g}_{Ca}$. Here, several cases closely related with the current work are shown in Figs. 15–17. In Fig. 14, the $\bar{g}_{K(ATP)}$ is changed to 10000 pS from the original value of 40000 pS. $\bar{g}_{Ca}$ is changed to 900 pS and 1100 pS from the original value of 1000 pS in Figs. 16 and 17, respectively.

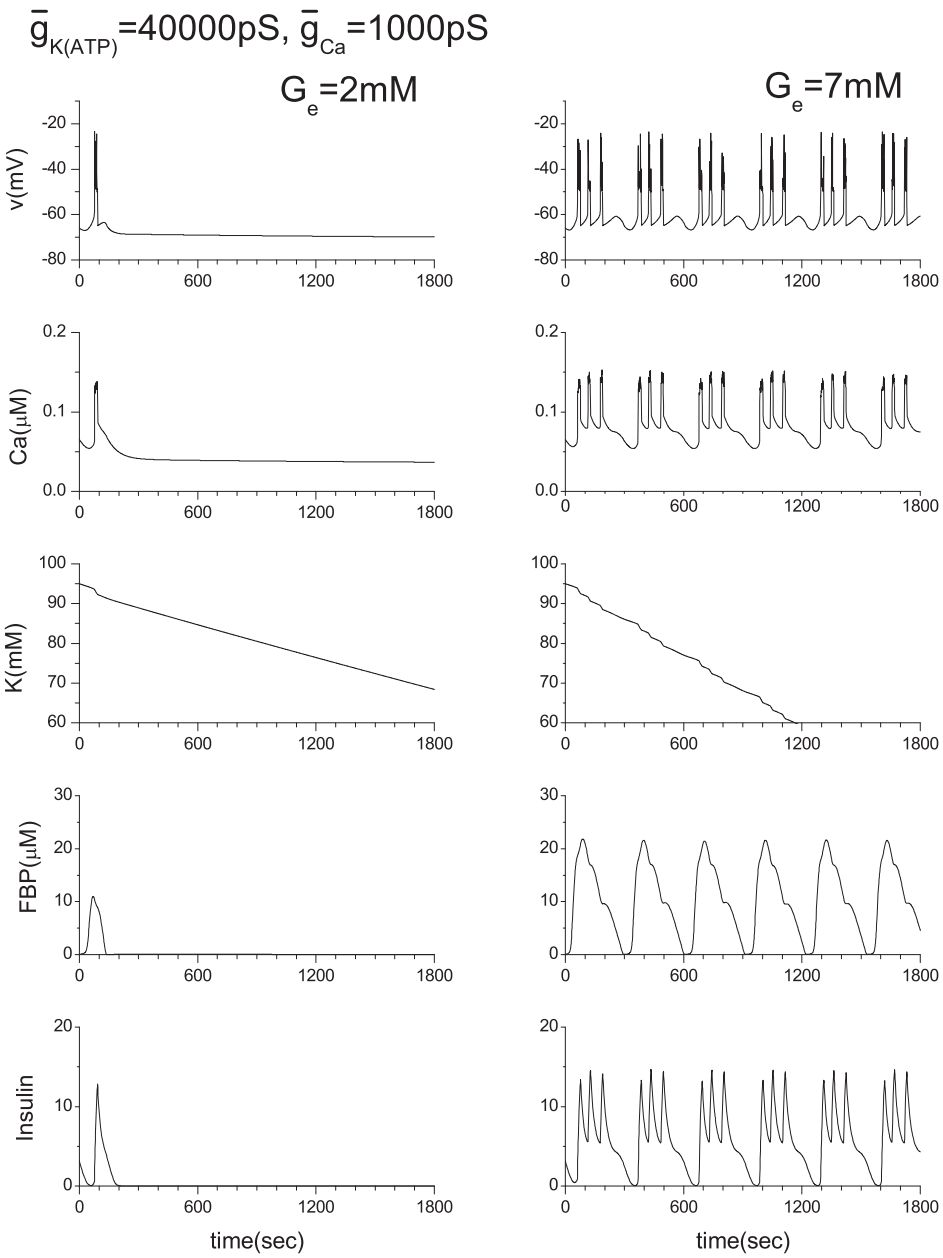

Figure 13 Single β-cell model calculations of Bedersen et al. together with Eq. (A3). The original model used the approximation of constant potassium ion concentration. Where v is the cell membrane potential, Ca is Ca^{2+} ion concentration, K is K^+ ion concentration, and FBP is the concentration of fructose 1,6-bisphosphate.

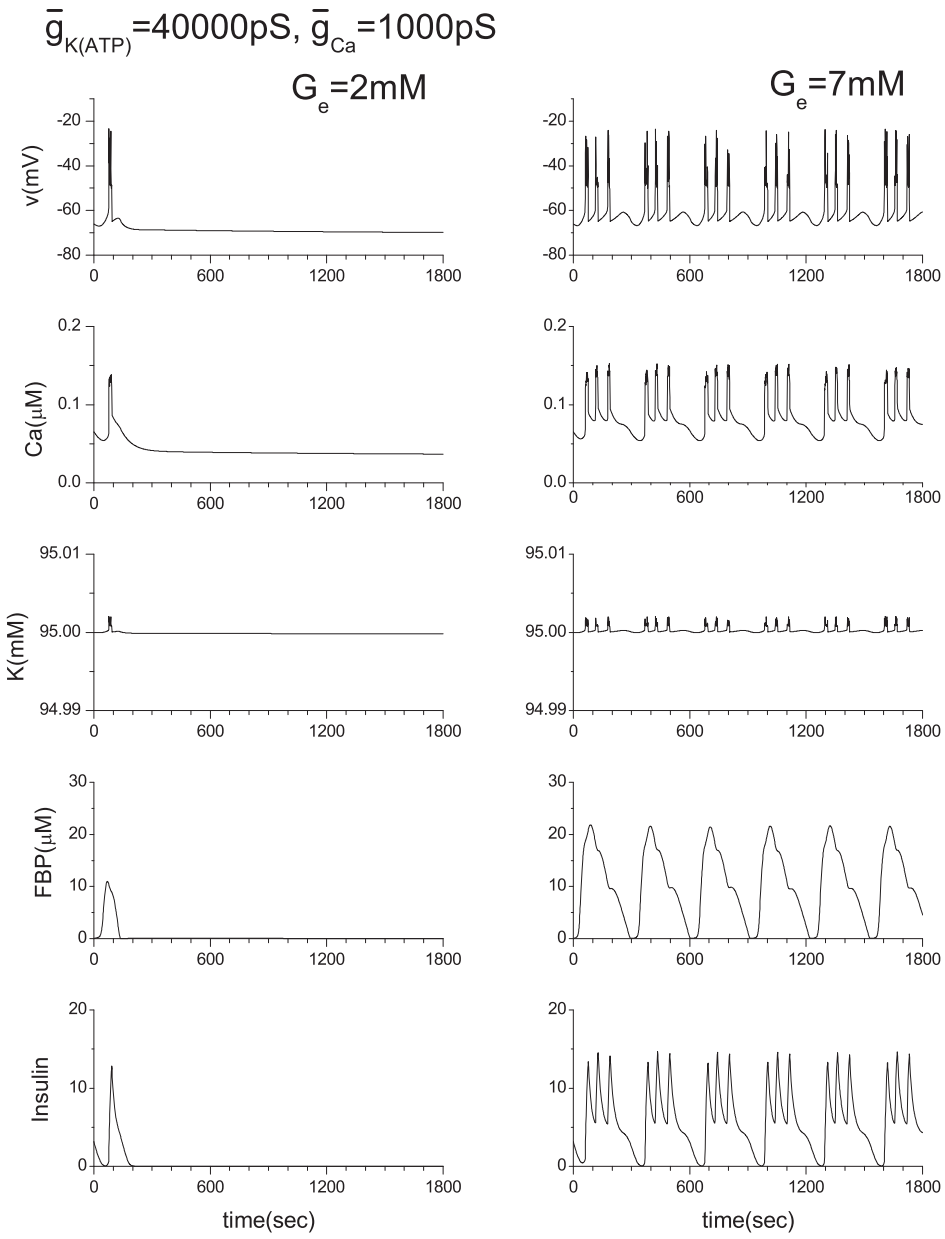

Figure 14 Modified single β-cell model calculations, where Eq. (A4) was used instead of Eq. (A3).

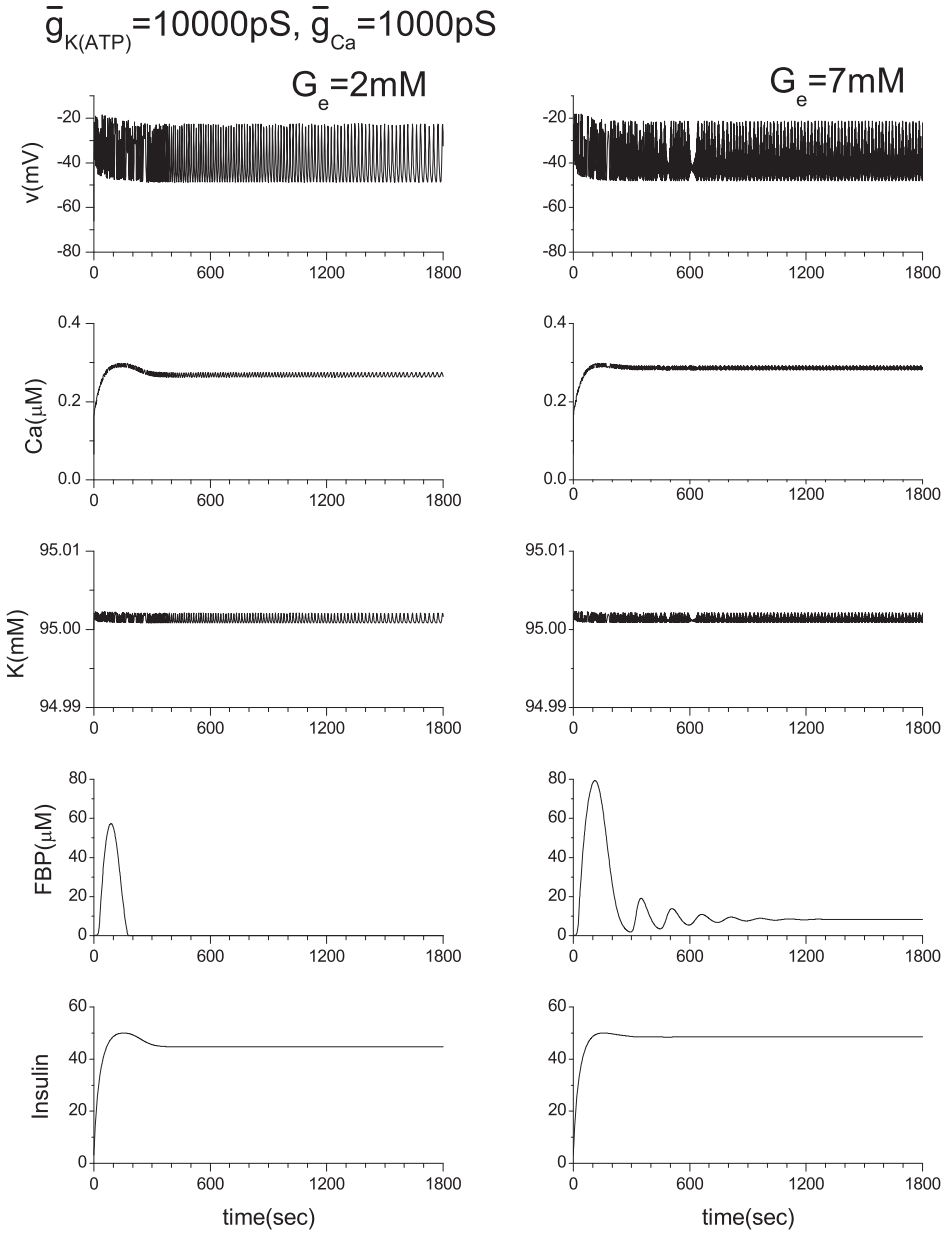

Figure 15 Effect of $\bar{g}_{K(ATP)}$ variation. Original $\bar{g}_{K(ATP)}$ value is 40000 pS. Note that K value is slightly higher than 95 mM here.

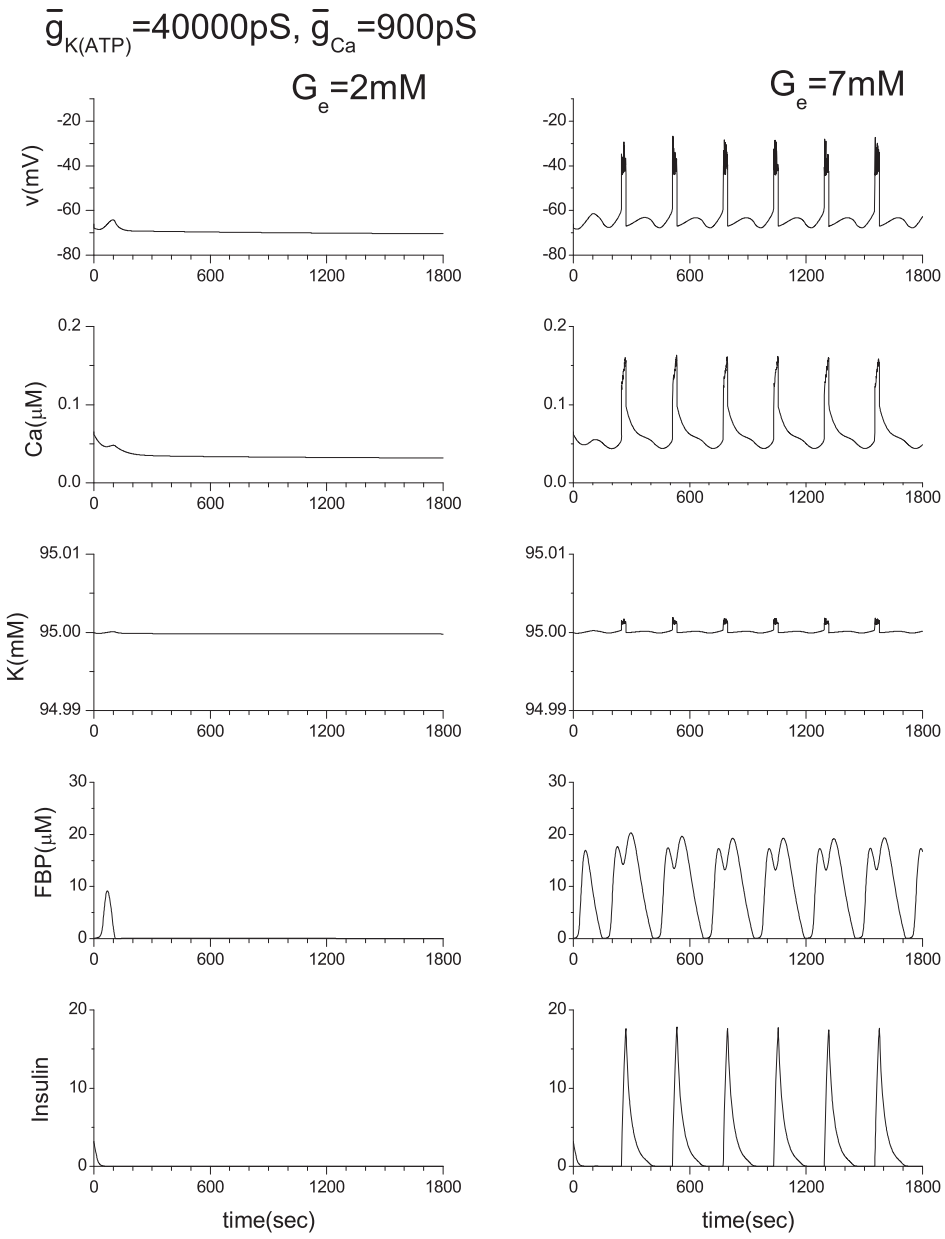

Figure 16 Effect of the $\bar{g}_{Ca}$ variation. Original $\bar{g}_{Ca}$ value is 1000 pS.

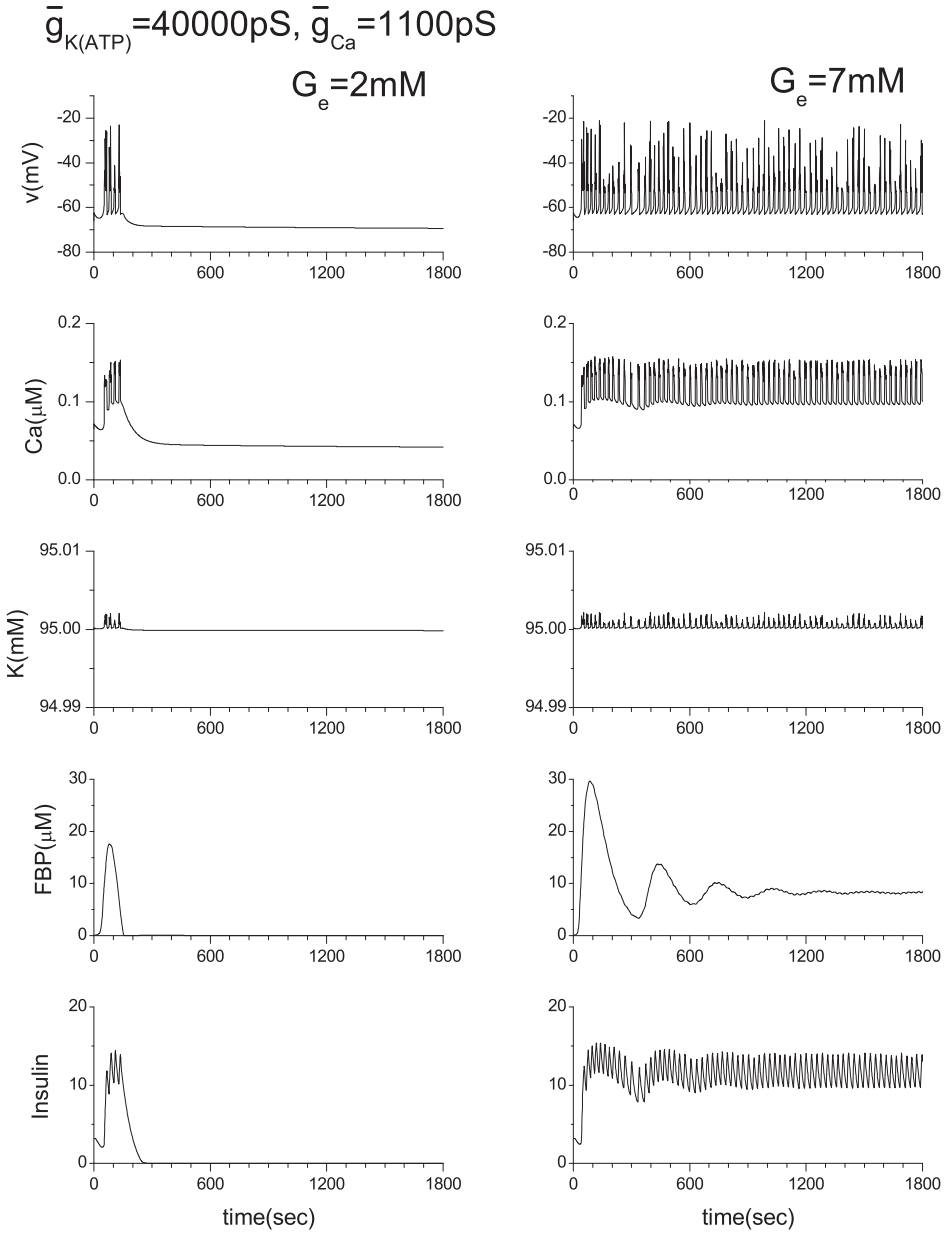

Figure 17 Effect of the $\bar{g}_{Ca}$ variation. Original $\bar{g}_{Ca}$ value is 1000 pS.